

Regge trajectories and resonances

5.1 Introduction

One of the most important conclusions of chapters 2 and 4 was that whenever a Regge trajectory, $\alpha(t)$, passes through a right-signature integral value of $J - v$ a t -plane pole will occur in the scattering amplitude because of the vanishing of the factor $\sin[\pi(\alpha(t) + \lambda')]$ in (4.6.2). And, as we found in section 1.5, such poles correspond to physical particles; to a particle which is stable against strong-interaction decays if the pole occurs below the t -channel threshold, or to a resonance which can decay into other lighter hadrons if it occurs above threshold. If a given trajectory passes through several such integers it will contain several particles of increasing spin, and so it is possible to classify the observed particles and resonances into families, each family lying on a given Regge trajectory. Some examples are given in figs. 5.5 and 5.6 below.

This chapter is mainly devoted to presenting the evidence for this Regge classification, but as there will be a different trajectory for each different set of internal quantum numbers such as B , I , S , etc. it will be useful for us first to examine briefly the way in which the particles have been classified according to their internal quantum numbers using $SU(3)$ symmetry and the quark model. Readers requiring a more complete discussion than we have space for here will find the books by Carruthers (1966), Gourdin (1967), and Kokkedee (1969) very helpful.

The complete specification of a hadron requires, in addition to its mass m , and spin σ , the values of the internal quantum numbers; i.e. baryon number B , charge Q , intrinsic parity $P = \eta\mathcal{P}$ from (4.6.8), strangeness S , and isospin I , and in some cases the charge conjugation C_n , and G -parity G , as well. All of these are good, conserved quantum numbers for strong interactions, though only B and Q are conserved in all interactions (to the best of our knowledge).

By definition $B = 0$ for mesons, $+1$ for baryons, and -1 for anti-baryons. These are the only values which occur for what are often loosely referred to as the 'elementary' particles (though see section 2.8 for a discussion of the more strict use of this terminology which we

employ). But baryon number is an additive quantum number, which means that a two-particle state $|1, 2\rangle$ will have baryon number $B_{12} = B_1 + B_2$, and so complex nuclei have $B = A$, the atomic mass number.

The intrinsic parity of a particle is $P = \pm 1$ depending on how its wave function transforms under the parity reflection operator in the particle's rest frame, i.e. $P_{\text{op}}\psi(\mathbf{r}) = \psi(-\mathbf{r}) = P\psi(\mathbf{r})$. This is a multiplicative quantum number, and so for a two-particle state $P_{12} = P_1 P_2 (-1)^l$, where l is the relative orbital angular momentum of the two particles (see (4.6.6)).

The charge-conjugation operator C , has the effect of turning a particle into its anti-particle, i.e. a particle which has the opposite sign for all the additive quantum numbers. So under C , $B \rightarrow -B$, $Q \rightarrow -Q$ and $S \rightarrow -S$. Since strong interactions are invariant under C , particles which have $B = Q = S = 0$, i.e. non-strange, neutral mesons, are eigenstates of C with eigenvalue $C_n = +1$ ($n \equiv$ neutral). It is found (see for example Bernstein (1968)) that $C_n = \pm 1$ for π^0 and η^0 , and $C_n = -1$ for ρ^0 , ω , ϕ and the photon γ . These assignments are consistent with the observed decays $\pi^0, \eta^0 \rightarrow \gamma\gamma$ and $\rho^0, \omega, \phi \rightarrow \gamma_\nu \rightarrow e^+e^-$ (where γ_ν is a virtual photon).

For other non-strange mesons ($B = S = 0$, $Q \neq 0$) it is useful to invoke the isospin invariance of strong interactions to define an extended particle-anti-particle conjugation operator called the G -parity operator. For such particles the z component of the isospin (see (5.2.1) below) is equal to the charge, i.e. $Q = I_z$, and so rotation of the particle state by an angle π about the y axis in 'isospin space' takes us to the charge-conjugate particle, i.e. $I_z \rightarrow -I_z$, up to a phase factor. The Condon and Shortley phase convention for isospin multiplets gives (cf. (B.7))

$$e^{i\pi I_y} |I, I_z\rangle = (-1)^{I-I_z} |I, -I_z\rangle \quad (5.1.1)$$

So for non-strange mesons the combined operation

$$G \equiv C e^{i\pi I_y} \quad (5.1.2)$$

will have an eigenvalue $G = \pm 1$. Thus for the pion multiplet, π^+ , π^0 , π^- , with $I = 1$, $I_z = 1, 0, -1$, we have $G_\pi = -1$ since $C_{\pi^0} = +1$. This is obviously also a multiplicative quantum number, and hence a state consisting of n pions will have $G|n\rangle = (-1)^n |n\rangle$. This allows one to determine the G -parity of other non-strange mesons from their hadronic decays into pions; for example the fact that the decay $\rho \rightarrow \pi\pi$

occurs indicates that ρ has $G = +1$. And of course the decays $\rho \rightarrow 3\pi$, 5π etc. are forbidden by G -parity conservation.

The remaining quantum numbers I and S require a brief discussion of unitary symmetry, which we give in the next section.

5.2 Unitary symmetry

a. Isospin

It is well known from nuclear physics that the strong interaction is approximately invariant under the transformations of the isotopic spin (or isospin) group $SU(2)$, at least to an accuracy of a few per cent. This group is isomorphic to the rotation group, the isospin vector I corresponding to J , while its z component in isospin space I_z corresponds to J_z . This isospin invariance manifests itself in two related ways.

(i) All the hadrons may be grouped conventionally into multiplets of a given isospin I (such that $I(I+1)$ is the eigenvalue of I^2) which are approximately degenerate in mass, and are identical in all their other quantum numbers except the charge. Well known examples are

Nucleon, N	p, n	$I = \frac{1}{2}, I_z = \pm \frac{1}{2}$
Pion, π	π^+, π^0, π^-	$I = 1, I_z = 1, 0, -1$
3-3 resonance, Δ	$\Delta^{++}, \Delta^+, \Delta^0, \Delta^-$	$I = \frac{3}{2}, I_z = \frac{3}{2}, \frac{1}{2}, -\frac{1}{2}, -\frac{3}{2}$

The isospin is assigned according to the multiplicity of charge states exhibited by the particle, so that I_z spans the range $I, I-1, \dots, -I$, and the z component is associated with the charge according to the relation

$$Q = I_z + \frac{1}{2}B \quad (5.2.1)$$

(for non-strange particles only). A particle may thus be represented by the isotopic state vector $|I, I_z\rangle$.

The mass differences within a given multiplet are rather small (for example $m_p = 938.3 \text{ MeV}$, $m_n = 939.6 \text{ MeV}$) and are believed to be caused by the differing electromagnetic interactions of the particles. As far as strong interactions are concerned such differences can be ignored, and so we use a single symbol for all the members of a multiplet (for example $N \equiv \{p, n\}$), and regard them all as lying on the same Regge trajectory, which carries a definite isospin. For example $\alpha_N(t)$ has $I = \frac{1}{2}$, and only if we want to discuss electromagnetic interactions need we take account of the fact that this is really two trajectories, with $I_z = \pm \frac{1}{2}$, which are very slightly split.

(ii) The various scattering amplitudes involving these particles are related by isospin invariance, being dependent on the value of I but not on I_z , i.e. strong interactions exhibit charge independence. This property will be examined in section 6.7.

It is sometimes convenient to regard the iso-doublet

$$(p, n) \quad |I = \frac{1}{2}, I_z = \pm \frac{1}{2}\rangle$$

as the fundamental isotopic spinor, out of which all other multiplets can be constructed (just as all possible angular momenta can be obtained by adding different numbers of spin = $\frac{1}{2}$ particles). This doublet iso-spinor can be represented by a column matrix.

$$\{2\} \equiv \eta \equiv \begin{pmatrix} p \\ n \end{pmatrix} \quad (5.2.2)$$

which transforms under $SU(2)$ as

$$\eta \rightarrow \eta' = \mathbf{U}\eta \quad (5.2.3)$$

where \mathbf{U} is any 2×2 unitary matrix with $\det(\mathbf{U}) = 1$. Any such matrix can be written in the form

$$\mathbf{U} = e^{i\theta \mathbf{n} \cdot \boldsymbol{\tau}} \quad (5.2.4)$$

where θ is an arbitrary parameter, \mathbf{n} is a unit three-vector, and the components of $\boldsymbol{\tau}$ are the Pauli matrices

$$\tau_x = \begin{pmatrix} 0 & 1 \\ 1 & 0 \end{pmatrix}, \quad \tau_y = \begin{pmatrix} 0 & -i \\ i & 0 \end{pmatrix}, \quad \tau_z = \begin{pmatrix} 1 & 0 \\ 0 & -1 \end{pmatrix} \quad (5.2.5)$$

The corresponding 'anti-particles' are given by the row-matrix iso-spinor

$$\{\bar{2}\} \equiv \bar{\eta} \equiv (\bar{p}, \bar{n}) \quad (5.2.6)$$

Formally all the other iso-multiplets can be constructed by combining η 's and $\bar{\eta}$'s. Thus for example

$$\frac{1}{\sqrt{2}}(\bar{p}p + \bar{n}n) \quad (5.2.7)$$

gives an $I = 0$ singlet, like the η meson, $\{1\}$, while

$$\bar{p}\bar{n}, \quad \frac{1}{\sqrt{2}}(\bar{p}p - \bar{n}n), \quad \text{and} \quad \bar{p}n \quad (5.2.8)$$

form the triplet, $\{3\}$, $I = 1$, $I_z = 1, 0, -1$ respectively, like the π meson. So at least in this formal sense we can regard the η and π mesons as bound states of the nucleon-antinucleon system, with

$$\{2\} \otimes \{2\} = \{1\} \oplus \{3\} \quad (5.2.9)$$

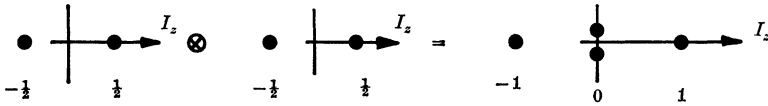


FIG. 5.1 The superposition of two iso-doublets, $I_z = \pm \frac{1}{2}$ to give four states, one with $I_z = -1$, two with $I_z = 0$ and one with $I_z = 1$.

as shown in fig. 5.1, completely in analogy with the construction of spin = 0 and spin = 1 helium atom states from two electrons of spin $\frac{1}{2}$.

b. SU(3)

The above scheme can be extended to include strange particles as well as by taking the fundamental representation to be the three-component spinor

$$\{\mathbf{3}\} \equiv \mathbf{q} \equiv \begin{pmatrix} p \\ n \\ \lambda \end{pmatrix} \quad (5.2.10)$$

transforming under SU(3) as

$$\mathbf{q} \rightarrow \mathbf{q}' = \mathbf{U}\mathbf{q} \quad (5.2.11)$$

where now \mathbf{U} is any unitary 3×3 matrix with $\det(\mathbf{U}) = 1$, which can be written

$$U = e^{\frac{1}{2}i\theta\alpha \cdot \lambda} \quad (5.2.12)$$

where α is an 8-dimensional unit vector, and the λ matrices are given in table 5.1. They correspond to the three τ matrices of SU(2), (5.2.5).

The three particles p , n , λ were introduced by Gell-Mann (1964) and Zweig (1964), and are called 'quarks'. They are assigned the quantum numbers shown in table 5.2. Clearly, the p and n quarks are not to be identified with the proton and neutron of (5.2.2) as they have, *inter alia*, $B = \frac{1}{3}$. We also need a triplet of anti-quarks

$$\{\bar{\mathbf{3}}\} \equiv \bar{\mathbf{q}} = (\bar{p}, \bar{n}, \bar{\lambda}) \quad (5.2.13)$$

There is no evidence that such quarks actually exist, but at the very least they provide a very convenient mnemonic for the group-theory of SU(3). Also the observed hadrons frequently behave as though they were actually composed of quarks as we shall discuss particularly in chapter 7. (An extensive review of the evidence for the quark structure of hadrons in electromagnetic and weak interactions is given in Feynman (1972).)

A baryon is made up of three quarks (to give $B = 1$), while mesons are composed of quark-antiquark pairs. The hypercharge, Y , is defined

Table 5.1 *The λ matrices of SU(3)*

$\lambda_1 = \begin{pmatrix} 0 & 1 & 0 \\ 1 & 0 & 0 \\ 0 & 0 & 0 \end{pmatrix}$	$\lambda_2 = \begin{pmatrix} 0 & -i & 0 \\ i & 0 & 0 \\ 0 & 0 & 0 \end{pmatrix}$
$\lambda_3 = \begin{pmatrix} 1 & 0 & 0 \\ 0 & -1 & 0 \\ 0 & 0 & 0 \end{pmatrix}$	$\lambda_4 = \begin{pmatrix} 0 & 0 & 1 \\ 0 & 0 & 0 \\ 1 & 0 & 0 \end{pmatrix}$
$\lambda_5 = \begin{pmatrix} 0 & 0 & -i \\ 0 & 0 & 0 \\ i & 0 & 0 \end{pmatrix}$	$\lambda_6 = \begin{pmatrix} 0 & 0 & 0 \\ 0 & 0 & 1 \\ 0 & 1 & 0 \end{pmatrix}$
$\lambda_7 = \begin{pmatrix} 0 & 0 & 0 \\ 0 & 0 & -i \\ 0 & i & 0 \end{pmatrix}$	$\lambda_8 = \begin{pmatrix} 1/\sqrt{3} & 0 & 0 \\ 0 & 1/\sqrt{3} & 0 \\ 0 & 0 & -2/\sqrt{3} \end{pmatrix}$

Table 5.2 *The quantum numbers of the quarks*

	<i>B</i>	<i>I</i>	<i>I_z</i>	<i>Q</i>	<i>S</i>	<i>Y</i>
p	$\frac{1}{3}$	$\frac{1}{2}$	$\frac{1}{2}$	$\frac{2}{3}$	0	$\frac{1}{3}$
n	$\frac{1}{3}$	$\frac{1}{2}$	$-\frac{1}{2}$	$-\frac{1}{3}$	0	$\frac{1}{3}$
λ	$\frac{1}{3}$	0	0	$-\frac{1}{3}$	-1	$-\frac{2}{3}$

in terms of the strangeness *S* by

$$Y = S + B \tag{5.2.14}$$

and the charge is then given by the Gell-Mann-Nishijima relation

$$Q = I_z + \frac{1}{2}Y = I_z + \frac{1}{2}(S + B) \tag{5.2.15}$$

instead of (5.2.1).

Taking all possible combinations of a quark and an antiquark, as shown in fig. 5.2, we get

$$q\bar{q} = \{3\} \otimes \{\bar{3}\} = \{1\} \oplus \{8\} \tag{5.2.16}$$

so we can expect that mesons will occur in nonets, each nonet consisting of a singlet and an octet with the quantum numbers shown in fig. 5.2. Table 5.3 gives the well established mesons grouped into such multiplets. It is evident that the symmetry is very badly broken for the masses of the particles, the SU(3) mass-splitting in *Y* being very much greater than the isospin mass-splitting in *I_z*.

Also it is not clear how one should distinguish the singlet states such as ω_1 from the octet state with the same quantum numbers, ω_8 . With a broken symmetry the observed ω and ϕ particles can be

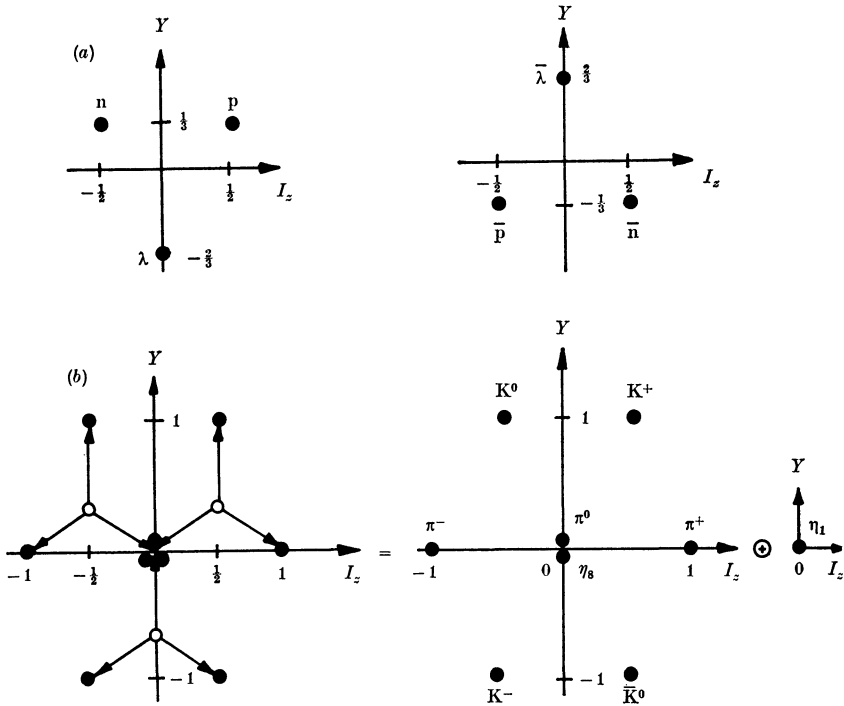


FIG. 5.2 (a) Triplets of quarks $\{p, n, \lambda\}$ and anti quarks $\{\bar{p}, \bar{n}, \bar{\lambda}\}$. (b) The decomposition $q \otimes \bar{q} = \{8\} + \{1\}$. On each quark represented by \circ is imposed an anti-quark triplet to give the nine states which are identified with pseudo-scalar mesons on the right-hand side.

mixtures of these pure $SU(3)$ states, say

$$\left. \begin{aligned} \phi &= \omega_8 \cos \theta - \omega_1 \sin \theta \\ \omega &= \omega_8 \sin \theta + \omega_1 \cos \theta \end{aligned} \right\} \quad (5.2.17)$$

where θ is the 'mixing angle'. The so-called 'ideal' value is

$$\theta = \tan^{-1} \left(\frac{1}{\sqrt{2}} \right) \approx 38^\circ \quad (5.2.18)$$

in which case from table 5.3 we find that

$$\omega = \frac{1}{\sqrt{2}} (p\bar{p} + n\bar{n}), \quad \phi = -\lambda\bar{\lambda} \quad (5.2.19)$$

so that ω contains no strange quarks. This ideal mixing seems to hold for the vector and tensor mesons, but not the pseudo-scalars.

The mass separations within a given multiplet are assumed to be

Table 5.3 *Meson nonets and their quark content*

Multi-plet	Quark content	Particles J^{PC}_n							
		I	S	0^{-+} PS	1^{-+} V	0^{++} S	1^{++} A^+	1^{+-} A^-	2^{++} T
{8}	$p\bar{n}$	1	0	π^+ (140)	ρ^+ (770)	δ^+ (970)	A_1^+ (1100)	B^+ (1235)	A_2^+ (1310)
	$\frac{1}{\sqrt{2}}(p\bar{p} - n\bar{n})$	1	0	π^0	ρ^0	δ^0	A_1^0	B^0	A_2^0
	$n\bar{p}$	1	0	π^-	ρ^-	δ^-	A_1^-	B^-	A_2^-
	$n\bar{\lambda}$	$\frac{1}{2}$	1	K^0 (498)	K^{*0} (890)	κ^0 (1300)	Q^0 (1240)	Q^0 (1280)	K^{*0} (1420)
	$p\bar{\lambda}$	$\frac{1}{2}$	1	K^+	K^{*+}	κ^+	Q^0	Q^0	K^{*+}
	$\lambda\bar{n}$	$\frac{1}{2}$	-1	\bar{K}^0	\bar{K}^{*0}	$\bar{\kappa}^0$	\bar{Q}^0	\bar{Q}^0	\bar{K}^{*0}
	$\lambda\bar{p}$	$\frac{1}{2}$	-1	K^-	K^{*-}	κ^-	Q^-	Q^-	K^{*-}
	$\frac{1}{\sqrt{6}}(p\bar{p} + n\bar{n} - 2\lambda\bar{\lambda})$	0	0	η_8	ω_8	ε_8	D_8	H_8	f_8
{1}	$\frac{1}{\sqrt{3}}(p\bar{p} + n\bar{n} + \lambda\bar{\lambda})$	0	0	η_1	ω_1	ε_1	D_1	H_1	f_1

All the particles in the PS, V and T nonets are well established, but some of the others are less certain. Masses (in MeV) have been given only for the first member of each isospin multiplet. C_n is not a good quantum number for strange mesons so the assignment in the Q region is particularly uncertain. The isosinglet mixtures are $\eta_8 + \eta_1 = \eta(549) + \eta'(958)$, $\omega_8 + \omega_1 = \omega(783) + \phi(1019)$, $\varepsilon_8 + \varepsilon_1 = \varepsilon(600) + S^*(993)$, $D_8 + D_1 = D(1285) + E(1420)$, $H_8 + H_1 = H(990) + ?$, $f_8 + f_1 = f(1270) + f'(1514)$, mixed as in (5.2.17).

due to the λ quark having a different mass from that of the p and n quarks. So with ideal mixing, if we set $m_n = m_p = m$ and $m_\lambda = m + \Delta m$, we find that for the vector mesons

$$m_\omega = m_\rho = 2m, \quad m_{K^*} = 2m + \Delta m, \quad m_\phi = 2(m + \Delta m) \quad (5.2.20)$$

giving
$$m_\omega + m_\phi = 2m_{K^*} \quad (5.2.21)$$

However for mesons it is generally supposed (for no very compelling reason) that these relations should actually be written for the squares of the masses, i.e. $m_\omega^2 = m_\rho^2$, $m_\omega^2 + m_\phi^2 = 2m_{K^*}^2$, which hold equally well because the masses are much larger than the mass differences. The lighter pseudo-scalar mesons do not obey the corresponding mass formulae either for m or m^2 , which is generally taken as evidence that the mixing between η and η' is far from ideal (see Kokkedee 1969).

Both the pseudo-scalar (PS) and vector (V) meson nonets can be

obtained with the spin = $\frac{1}{2}$ quarks in an $l = 0$ orbital state, since they correspond to quark spins being anti-parallel (total quark spin $s = 0$) or parallel ($s = 1$) respectively. Higher spin mesons can be obtained by orbital excitation of the $q\bar{q}$ pair. Since q and \bar{q} , being fermions, have opposite intrinsic parity, the parity of a $q\bar{q}$ state is

$$P = (-1)^{l+1} \quad (5.2.22)$$

and for $B = S = 0$ states the charge conjugation and G -parity are

$$C_n = (-1)^{l+s}, \quad G = (-1)^{l+s+I} \quad (5.2.23)$$

Since the spin of the meson is $J = l + s$ we have for $l = 0$ just the PS and V nonets with $J^{PC} = 0^{-+}$ and 1^{--} respectively, while for $l = 1$ there are four possible nonets, scalar $S \equiv 0^{++}$, two axial vectors, $A^+ \equiv 1^{+-}$ and $A^- \equiv 1^{-+}$, and tensor $T \equiv 2^{++}$. A possible assignment of meson states according to this classification is given in table 5.3.

Regge theory suggests that one may expect to see recurrences of each of these six nonets at J values spaced by 2 units from the above. In the next section we shall find that only a few of these excited states have been observed. This is hardly surprising, however, because mesons can usually only be observed in production experiments such as

$$1 + 2 \rightarrow 3 + 4, \quad 4 \rightarrow a + b$$

The resonance 4 will be seen as a peak of the cross-section in the invariant mass of its decay products at $m_4^2 = (p_a + p_b)^2$, a and b having an angular distribution corresponding to the spin of 4 (see section 4.2). But at high values of m_4^2 many partial waves can be expected to contribute to the ab system and so the analysis of this decay within the three-body final state $3 + a + b$ becomes difficult. Un-natural parity mesons are even more difficult to find as they only have three (or more) body decays.

The situation is more favourable for baryon resonances which can be formed in meson-baryon scattering experiments such as

$$MB \rightarrow B^* \rightarrow MB$$

where a partial-wave analysis of the two-body final state is sufficient to find the resonance. So a lot more baryon resonances are known.

They are built from three quarks

$$q \otimes q \otimes q = \{3\} \otimes \{3\} \otimes \{3\} = \{1\} \oplus \{8\} \oplus \{8\} + \{10\} \quad (5.2.24)$$

(see Carruthers 1966), and so baryons should occur in singlets, octets and decuplets, with the quantum numbers shown in fig. 5.3

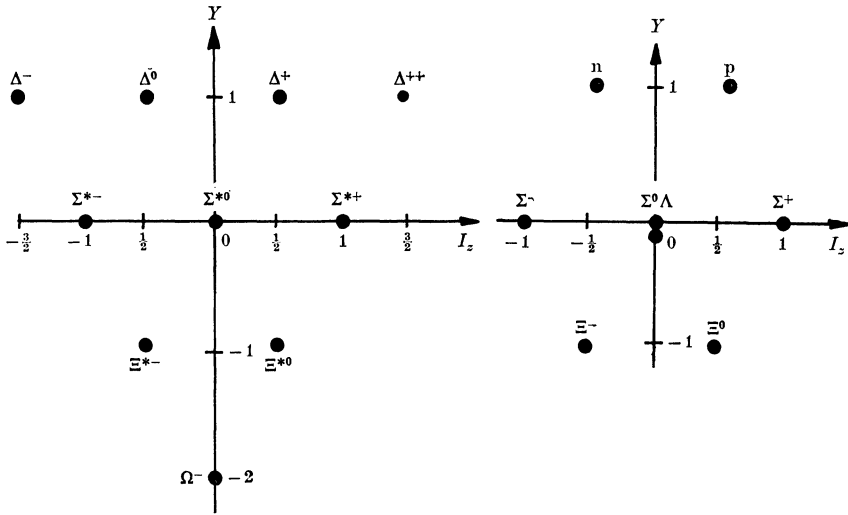


FIG. 5.3 The $J^P = \frac{3}{2}^+$ decouplet and the $\frac{1}{2}^+$ octet of baryons.

The lowest mass states, with $l = 0$ may have $J = \frac{1}{2}$ or $\frac{3}{2}$, and are given in table 5.4, and again one may expect higher l states at higher masses. (We shall ignore the difficulty that since the quarks are fermions with presumably anti-symmetric wave functions the increase of mass with J is far from obvious—see Kokkedee (1969).) By the same method as before we find that the mass-splitting in the decouplet should obey the equal spacing rule

$$m_{\Omega^-} - m_{\Xi^*} = m_{\Xi^*} - m_{\Sigma^*} = m_{\Sigma^*} - m_{\Delta} = \Delta m \tag{5.2.25}$$

which is well satisfied. For the octet we obtain the Gell-Mann-Okubo mass formula

$$m_p + m_{\Xi} = \frac{1}{2}(m_{\Sigma} + 3m_{\Lambda}) \tag{5.2.26}$$

but the relations $m_{\Lambda} = m_{\Sigma}$ and $m_{\Lambda} - m_p = m_{\Sigma^*} - m_{\Delta}$ are not obeyed, so there must be symmetry-breaking effects in the potential between the quarks as well.

In addition to these predictions about the masses of the particles SU(3) invariance also gives relations between scattering amplitudes, and these will be explored in section 6.7.

The scheme outlined above is only the most elementary version of the quark model. The discovery of two long-lived vector mesons, ψ_1 (3100) and ψ_2 (3700) (see Particle Data Group (1975) for references) has increased the interest in more elaborate structures based on the inclusion of a fourth quark, c , having the quantum numbers

$$B, Q, I, S, C = \frac{1}{3}, \frac{2}{3}, 0, 0, 1,$$

Table 5.4 *The lowest mass octet and decuplet of baryons and their quark content*

Multiplet	Quark content	I	S	Particles	
$\{8\}, J^P = \frac{1}{2}^+$	ppn	$\frac{1}{2}$	0	p(938.3)	
	pnn	$\frac{1}{2}$	0	n(939.6)	
	pp λ	1	-1	$\Sigma^+(1189.5)$	
	pn λ	1	-1	$\Sigma^0(1192.6)$	
		0	-1	$\Lambda(1115.6)$	
	nn λ	1	-1	$\Sigma^-(1197.4)$	
	p $\lambda\lambda$	$\frac{1}{2}$	-2	$\Xi^0(1314.7)$	
	n $\lambda\lambda$	$\frac{1}{2}$	-2	$\Xi^-(1321.2)$	
	$\{10\}, J^P = \frac{3}{2}^+$	ppp	$\frac{3}{2}$	0	$\Delta^{++}(1236)$
		ppn	$\frac{3}{2}$	0	Δ^+
pnn		$\frac{3}{2}$	0	Δ^0	
nnn		$\frac{3}{2}$	0	Δ^-	
pp λ		1	-1	$\Sigma^{*+}(1383)$	
pn λ		1	-1	Σ^{*0}	
nn λ		1	-1	Σ^{*-}	
p $\lambda\lambda$		$\frac{1}{2}$	-2	$\Xi^{*0}(1532)$	
n $\lambda\lambda$		$\frac{1}{2}$	-2	Ξ^{*-}	
$\lambda\lambda\lambda$		0	-3	$\Omega^-(1672)$	

where C is a new quantum number called 'charm', which has eigenvalue 0 for the p, n and λ quarks. The particles ψ_1 and ψ_2 are taken to be $c\bar{c}$ bound states, and the basic meson SU(3) nonets from $\{3\} \otimes \{3\}$ are increased to SU(4) 16-plets formed from $\{4\} \otimes \{4\}$. However this fourth quark must be much heavier than the others so that the predicted charmed particles (formed from $c\bar{p}$, $c\bar{n}$, $c\bar{\lambda}$, $\bar{c}p$, $\bar{c}n$, $\bar{c}\lambda$) are heavier than the nonet mesons, whose SU(3) symmetry and mixing are approximately preserved. The discovery of charmed particles has greatly increased the interest of this model, and of the related schemes based on 'coloured' quarks (see Weinberg (1974), de Rujula *et al.* (1974), Gaillard, Lee and Rosner (1975) for reviews).

An important test of the quark model is that all the observed mesons have quantum numbers which can be formed from $q \otimes \bar{q}$ as in fig. 5.2, and all the baryons have quantum numbers that can be formed from $q \otimes q \otimes q$ as in fig. 5.3. Channels which have quantum numbers outside these patterns, like $\pi^+\pi^+$ which has $I = 2$, or K^+p which as $S = 1$, are called 'exotic' channels, and do not seem to contain resonances. All the well established resonances have non-exotic quantum numbers.

5.3 The Regge trajectories

An authoritative survey of the experimental properties of particles and resonances is published at frequent intervals by the Particle Data Group. Their 1974 edition (Particle Data Group 1974) contains information on over 50 possible mesons and 90 baryons, though the evidence for some of these is fairly weak. In this section we shall try to group all the particles for which there is reasonably strong evidence on Regge trajectories. Of course this cannot be done with complete certainty because there are few *a priori* rules to direct which particles should be associated together on the same trajectory. But, as we shall see, this problem is greatly simplified by the fact that the trajectories seem to be straight parallel lines when $\text{Re}\{\alpha(t)\}$ is plotted against t .

a. Mesons

All the well established mesons are shown in fig. 5.4 in a Chew-Frautschi plot (Chew and Frautschi 1962) of the spin $\sigma (= \text{Re}\{\alpha\})$ versus $\text{mass}^2 = t$. It should be noted that the only well verified particle with $\sigma > 2$ is the spin = 3, $I = 1$, g meson which has the same internal quantum numbers as the ρ ($\sigma = 1$) and so presumably lies on the same trajectory. Strictly this is the only trajectory on which we can put even two points! However, in drawing fig. 5.4 we have taken into account that there is also evidence for spin = 3 ω and K^* resonances and spin = 4 h and A_2^* resonances, and have made some use of information about the behaviour of the trajectories in the region $t < 0$ obtained from Regge fits (see fig. 6.6. below).

Also it is found that the $\sigma = 2$ A_2 meson, which has similar quantum numbers to the ρ apart from its signature (note from (4.6.8), (5.2.22) and (5.2.23) that this in fact means opposite values of P , C_n and G), lies very close to the straight line joining ρ and g, and (fig. 6.6) the A_2 trajectory is close to that of the ρ for $t < 0$ as well. Such an identity between trajectories of opposite signature is called 'exchange degeneracy'. It seems to imply (from (2.5.3) or (4.5.7)) that, rather surprisingly, the exchange forces, i.e. the u -channel singularities, are not making much contribution to the trajectories. Similarly the ω and f, which because of ideal mixing are almost degenerate in mass with the ρ and A_2 respectively (see (5.2.20)), seem to lie on a single $I = 0$ exchange-degenerate trajectory which almost coincides with that of ρ , A_2 , g while the $I = 0$, ϕ , f' trajectory appears to be parallel with these.

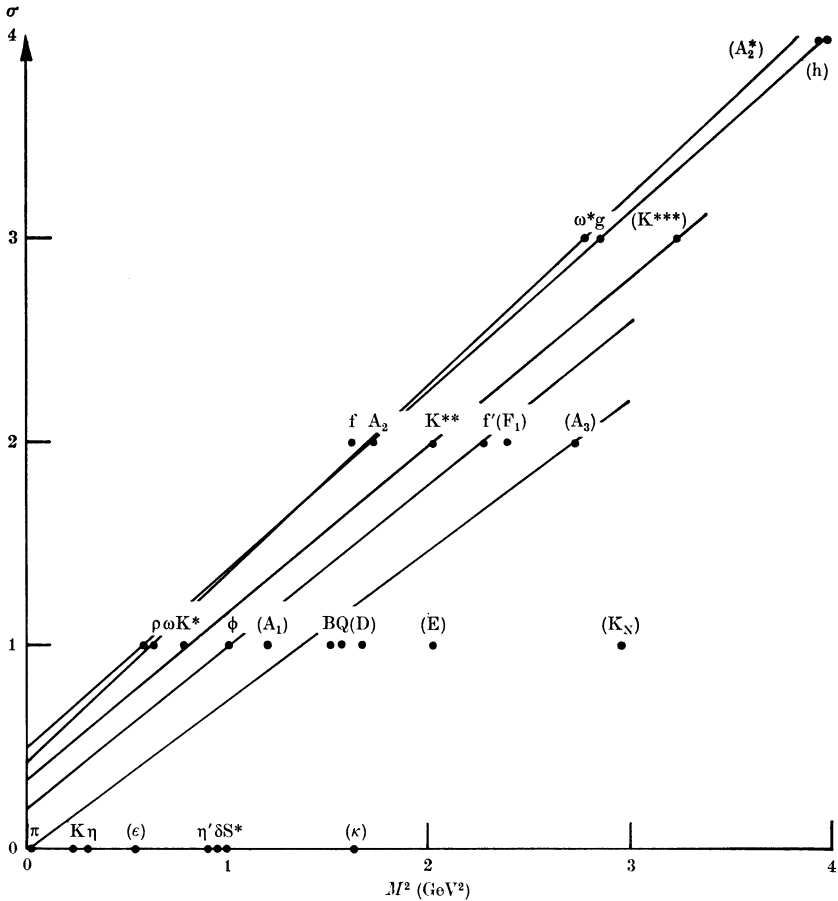


FIG. 5.4 Chew-Frautschi plot of $\text{Re}\{\alpha(t)\}$ versus t for the well established mesons. Less well verified states appear in brackets.

If we then make the rather bold assumption that all the mesons lie on approximately straight, parallel, exchange-degenerate trajectories we can associate most of the states listed by the Particle Data Group with trajectories as shown in fig. 5.5. They give leading trajectories which are very approximately

$$\left. \begin{aligned}
 \alpha_\rho(t) &\approx 0.5 + 0.9t & \rho, \omega, A_2, f, g, \omega^*, A_2^*, h & \quad I = 0, 1 \\
 \alpha_{K^*}(t) &\approx 0.3 + 0.9t & K^*, K^{**}, K^{***} & \quad I = \frac{1}{2} \\
 \alpha_\phi(t) &\approx 0.1 + 0.9t & \phi, f' & \quad I = 0 \\
 \alpha_\pi(t) &\approx 0.0 + 0.8t & \pi, B, A_3 & \quad I = 1 \\
 \alpha_K(t) &\approx -0.2 + 0.8t & K, Q, L & \quad I = \frac{1}{2}
 \end{aligned} \right\} \quad (5.3.1)$$

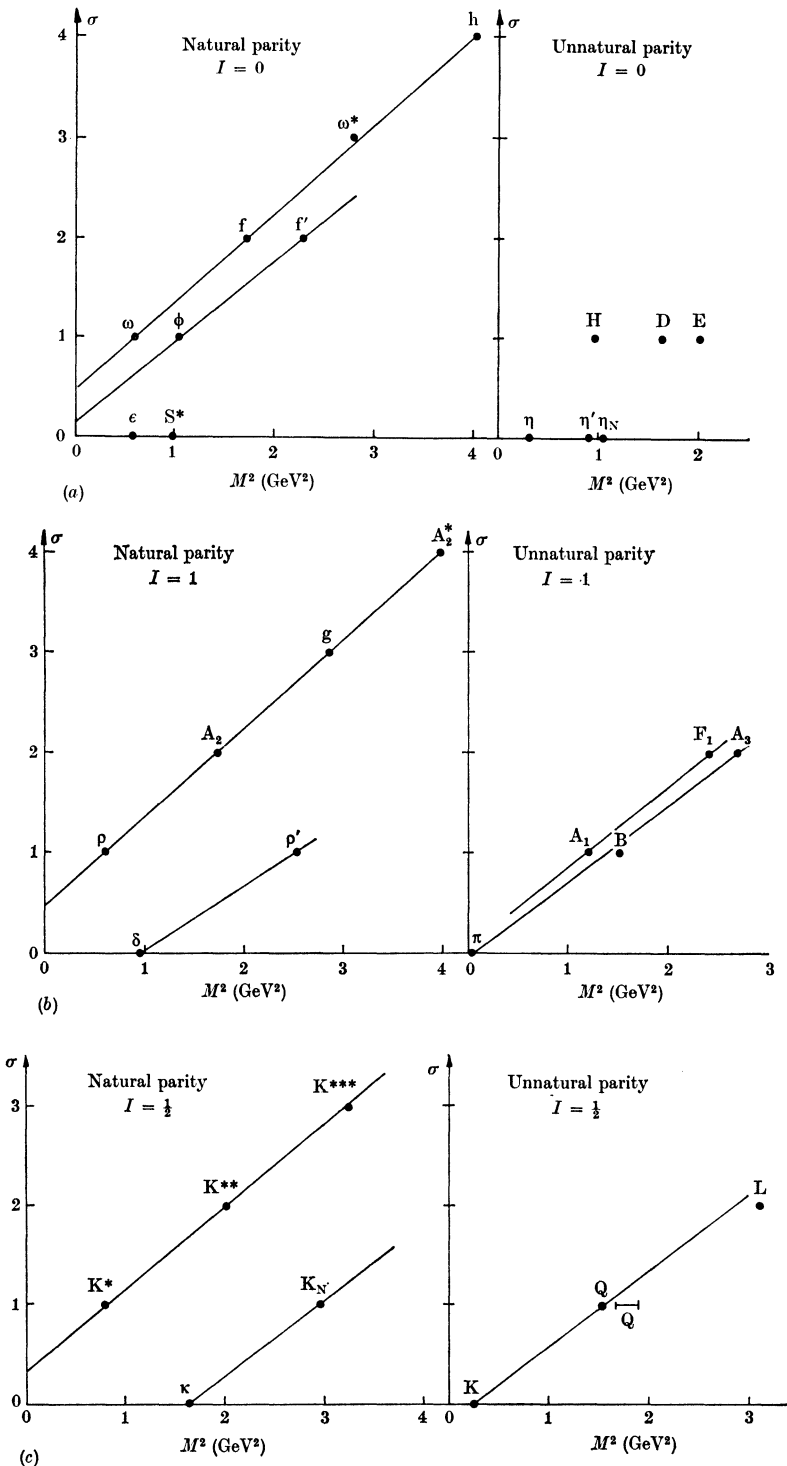


FIG. 5.5 Meson trajectories for (a) $I = 0$, (b) $I = 1$ and (c) $I = \frac{1}{2}$ mesons, including less well established states.

These straight lines are suggestive of a harmonic oscillator type of effective potential between the quarks, as mentioned in equation (3.3.33) *et seq.* An additional motivation for these figures, to be discussed in sections 6.5 and 7.4, is that there are theoretical reasons for expecting that trajectories may occur in integrally spaced sequences, with a ‘parent’ trajectory $\alpha(t)$, and an infinite sequence of ‘daughters’ $\alpha_n(t) \equiv \alpha(t) - n, n = 1, 2, \dots$. Thus the $\rho'(1600)$, if it really is a resonance, may lie on the $n = 2$ daughter of the ρ .

b. Baryons

There are many more baryon states with high spin whose quantum numbers have been fairly well determined, and so the Chew–Frautschi plots of figs. 5.6 are more highly populated.

Again the trajectories seem to be straight and parallel, with similar slopes to the meson trajectories, but exchange degeneracy is badly broken in many cases. The leading trajectories are approximately given by

$$\left. \begin{aligned} \alpha_N(t) &\approx -0.3 + 0.9t && N(939), N(1688), N(2220) \\ \alpha_\Delta(t) &\approx 0.0 + 0.9t && \Delta(1232), \Delta(1950), \Delta(2420), \Delta(2850), \Delta(3230) \\ \alpha_\Lambda(t) &\approx -0.6 + 0.9t && \Lambda(1116), \Lambda(1520), \Lambda(1815), \Lambda(2100), \Lambda(2350), \\ &&& \Lambda(2585) \\ \alpha_\Sigma(t) &\approx -0.8 + 0.9t && \Sigma(1190), \Sigma(1915) \end{aligned} \right\} \tag{5.3.2}$$

We have plotted the natural and unnatural parity trajectories back to back because the generalized MacDowell symmetry (see section 6.5) requires that odd-baryon-number trajectories should satisfy the relation

$$\alpha^+(\sqrt{t}) = \alpha^-(-\sqrt{t}), \quad \text{for } t > 0 \tag{5.3.3}$$

where the superscripts \pm refer to the parity. Since the trajectories (5.3.2) are approximately even in \sqrt{t} this gives

$$\alpha^\pm(\sqrt{t}) = \alpha^0 + \alpha't \tag{5.3.4}$$

for both parities, and so the resonances should appear in exchange-degenerate pairs. It is evident from fig. 5.6 that this relation is not in fact satisfied, It is discussed further in section 6.5.

It is clear from the above figures that the Chew–Frautschi plot provides a very useful way of classifying resonances in addition to SU(3).

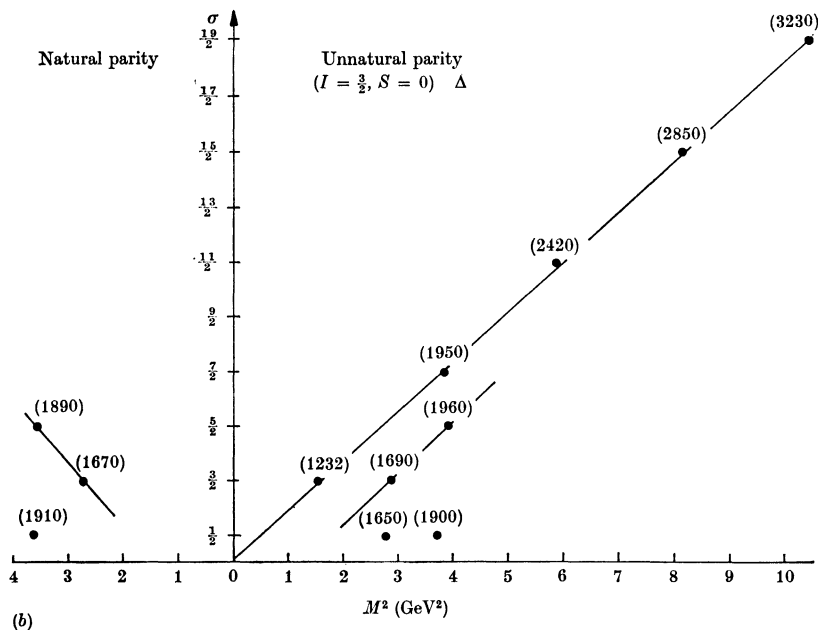
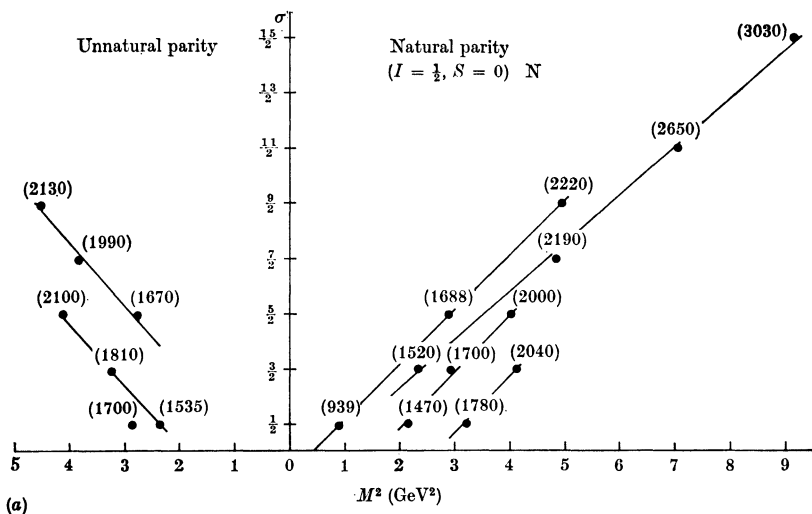
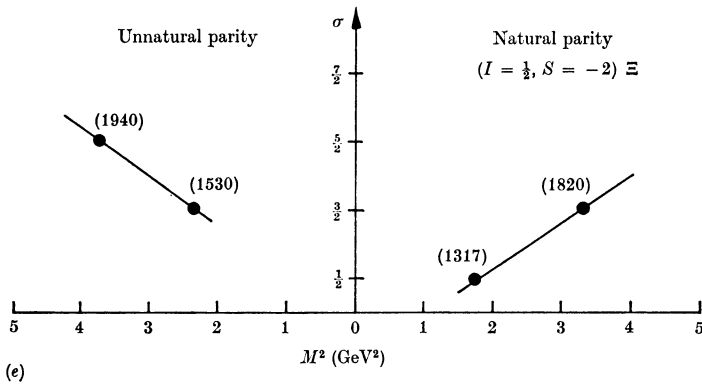
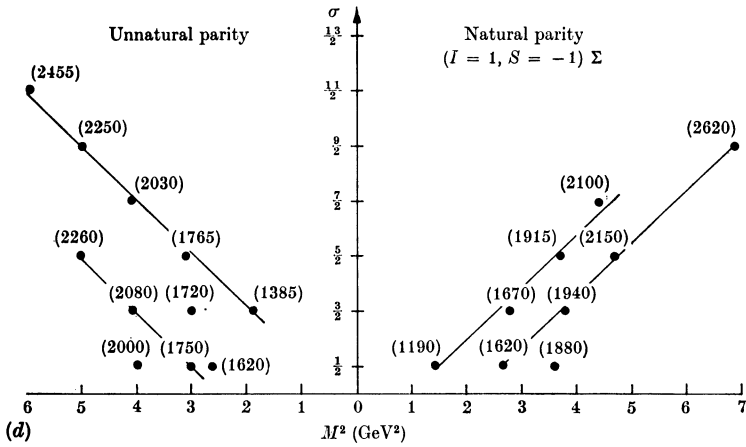
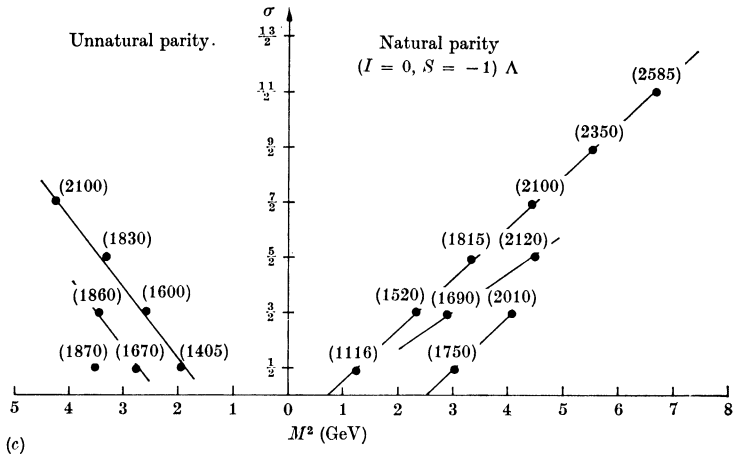


FIG. 5.6 Baryon trajectories for $(I, S) = (a) (\frac{1}{2}, 0), (b) (\frac{3}{2}, 0)$.



(c) $(0, -1)$, (d) $(1, -1)$ and (e) $(\frac{1}{2}, -2)$.

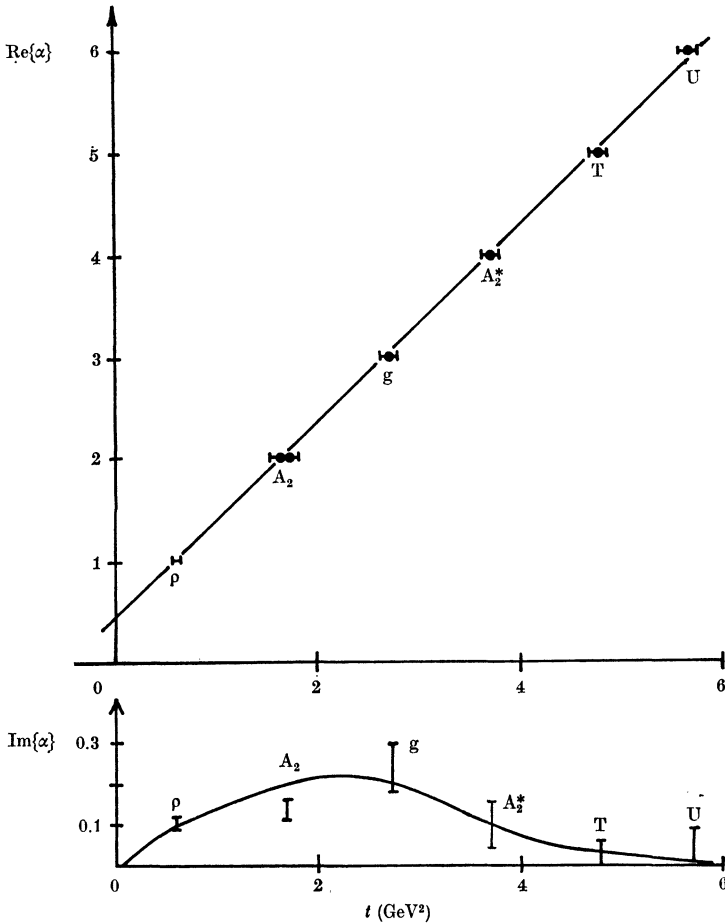


FIG. 5.7 A plot of $\text{Re} \{ \alpha(t) \}$ and $\text{Im} \{ \alpha(t) \}$ against t for the $I = 1$ ρ, A_2 exchange-degenerate trajectory.

5.4 The analytic properties of trajectories

The presence of external particles with spin does not alter significantly the conclusions drawn in section 3.2 about the analyticity of the Regge trajectory functions.

The position of a pole at $J = \alpha(t)$ is determined by (cf. (3.2.1))

$$(A_{HJ}(t))^{-1} \rightarrow 0 \quad \text{as } J \rightarrow \alpha(t) \tag{5.4.1}$$

so that usually $\alpha(t)$ will inherit only the singularities of $(A_{HJ}(t))^{-1}$. However, as discussed previously, $\alpha(t)$ will not obtain the left-hand cuts of the partial-wave amplitude. Also since the same trajectory

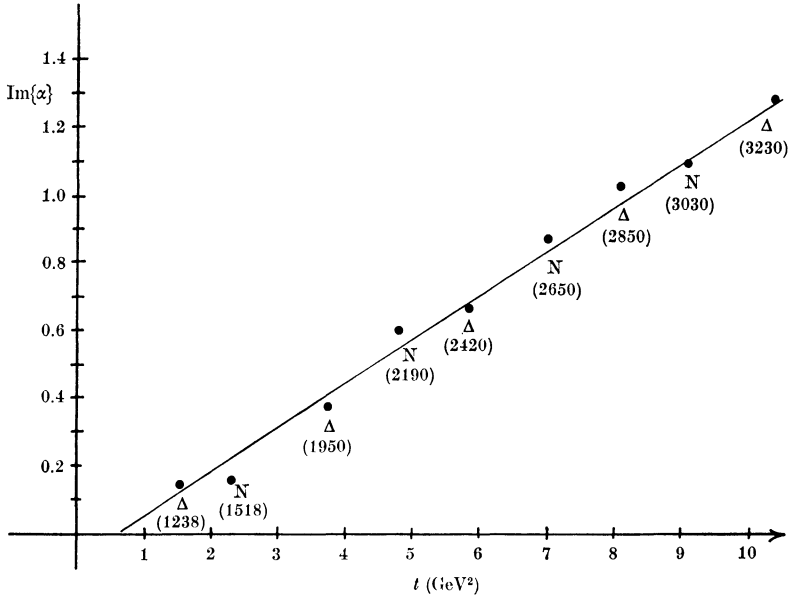


FIG. 5.8 A plot of $\text{Im}\{\alpha(t)\}$ against t for the N and Δ trajectories.

function occurs in all the different helicity amplitudes for a given process which are connected by the unitarity relation like (4.4.11), the various kinematical singularities of $A_{HJ}(t)$ which depend upon the helicities will not occur in $\alpha(t)$, though they are present in the Regge residue (see section 6.2).

So, unless trajectories cross each other, $\alpha(t)$ will have just the dynamical right-hand cut of $A_{HJ}(t)$ beginning at the t -channel threshold branch point, t_r . The unitarity relation (4.4.11) with (4.7.6) leads to the threshold behaviour

$$\text{Im}\{\alpha(t)\} \propto (t - t_r)^{\alpha(t_r) - \nu_{13}^+ + \frac{1}{2}}, \quad \alpha(t_r) - Y_{13}^+ > -\frac{1}{2} \quad (5.4.2)$$

instead of (3.2.26), and an infinite number of trajectories will accumulate at threshold at the point $J = Y_{13}^+ - \frac{1}{2}$, as in (3.2.29).

For mesons one can expect that the trajectory functions will satisfy dispersion relations like (3.2.12) or (3.2.13). But for baryons the MacDowell symmetry (5.3.3) implies that the dispersion relation must be written in terms of \sqrt{t} rather than t , so in unsubtracted form it reads

$$\alpha(\sqrt{t}) = \frac{1}{\pi} \int_{\sqrt{t_T}}^{\infty} \frac{\text{Im}\{\alpha(\sqrt{t'})\}}{\sqrt{t'} - \sqrt{t}} d\sqrt{t'} + \frac{1}{\pi} \int_{-\sqrt{t_T}}^{-\infty} \frac{\text{Im}\{\alpha(\sqrt{t'})\}}{\sqrt{t'} - \sqrt{t}} d\sqrt{t'} \quad (5.4.3)$$

where we have integrated over both the physical regions of $\alpha(\sqrt{t})$. Of course subtractions will in fact be necessary.

The magnitude of $\text{Im}\{\alpha(t)\}$ at the position of a resonance can be obtained from the width of that resonance using (2.8.7). The values obtained for the ρ trajectory are shown in fig. 5.7, and those for the N and Δ trajectories in fig. 5.8.

In each case $\text{Im}\{\alpha(t)\} \ll \text{Re}\{\alpha(t)\}$, which, together with the linearity of $\text{Re}\{\alpha(t)\}$ strongly suggests that the dispersion relation (3.2.12) holds, rather than (3.2.11) which is valid for potential scattering and the ladder models described in section 3.4. We shall discuss this point further in chapter 11.